Quartarly Journal of Technology & Education
Vol.1, Special issue. Autumn 2006

Comparison of TOF, FMCW and Phase-Shift Laser Range-Finding Methods by Simulation and Measurement

Shahram Mohammad Nejad
University of Science and Technology
shahramm@iust.ac.ir
Saeed Olyaee
Shahid Rajaee Teather Training Uaiersity
s_olyaee@srttu.edu

Abstract

Since 1970s the use of laser based range-finders has become a necessary part of many military and domestic systems. According to the needs and the circumstances, many different types of such systems have been developed and their technologies are adapted to the local needs. Distance or displacement measurement in the medium range is mainly divided to three groups; time of flight, frequency modulation continuous wave, and phase-shift laser range finder. In this paper we present the design, implementation and/or simulation of three such systems and compare their characteristics.

Keywords

Time-Of-Flight, Laser Range Finder, FMCW-Like distance measuring system, phase shift, heterodyne technique.

1. Introduction

Three major techniques are usually being used for range finding processes. These techniques are: Time of Flight (TOF), frequency modulation continuous wave (FMCW) and Phase-Shift [1-5]. The phase-shift and other techniques such as FMCW or the combination of interferrometry and phase-shift techniques could also be used to measure the intermediate distances with high accuracy [6-8]. But, none of these techniques could be used to measure distances above 1km, since in these techniques continuos wave (CW) or burst lasers are used.

On the other hand, to detect the reflecting beam from long distances, lasers having relatively high powers are required. Also, the use of high power lasers with continues wave or burst is impossible. Hence, for measuring distances above 1km, the use of pulsed lasers are necessary. As the repetition of the transmitter power increases, the system becomes complicated and also cooling becomes inevidable. If however, the repetition rate decreases, the detection of a moving target become very difficult. It is therfore necessary to compensate between the maximum distance to be measured, the repetition rate and the system's complication.

2- TOF Laser Range Finder

In a TOF laser range finding system, the round trip time measurement of a short powerful laser pulse is used to determine the distance [10-13]. With reducing the pulse width of the signal, the output power of the laser signal could be increased to several MW and the signal to noise ratio could also be increased considerably. The most important sections of a TOF system are:

a) The transmitting section including, the Q-switch, the HV source to drive the flash tube, the repetition rate controlling part, the cooling system and the transmitter optics.

b) The receiver analog section including, the APD detection parts, the low-noise and wide-band preamplifier, the converter, the limiter and the receiver optics.

c) The receiver digital section including, the isolating circuit, the processing and the interface circuits.

As can be seen from fig.1, the laser beam travels a distance of 2r. The received power is usually very small. The relation between the received power at the optic section, P_{inc}, and the distance r, is defined as [9]:

$$P_{inc} = \frac{\rho.\tau.S}{\pi.r^2} P_{opt} \quad , \qquad \tau = \tau_c.\tau_{opt} \tag{1}$$

where, τ is the transmitting coefficient (which is equal to the multiplication of transmitting coefficient of the optics and the transmitting coefficient of the media), ρ is the scattering coefficient of the target (ρ=1 for a perfect mirror and is equal to zero for a black body), P_{opt} is the laser output power and S is the receiver optic area. Considering a 1% for the target reflection and 75% for the transmission losses of the media, and assuming a perfectly round optical lens of 5cm radius, in a maximum distance of 20Km measurement by a 1.5MW laser source, the reflecting power will be 70.3nW only.

It can also be seen from fig.1 that, a **START** signal is simultaneously introduced to the processing circuit through a p-i-n diode. As the **START** is signal received, a counter is activated, until the **STOP** signal arrives. After travelling a distance of $2r$, the laser beam, trough the optics, arrives on the APD having high responsivity and a short rising time. In order to stop the counter, the APD photocurrent is converted into a voltage signal and is amplified. If the clock pulse frequency is f_{clk}, the distance between the target and the transmitter is,

$$r = \frac{C.N}{2f_{clk}} \tag{2}$$

where N accounts for the counted digits of the counter (between the START and the STOP signals) and C is the speed of light. In accordance to equation (2), the resolution of the system related to a clock pulse of the counter becomes,

$$\delta_r = \frac{C}{2f_{clk}} \tag{3}$$

The main function of the transmitting section is to produce a relatively powerful short period pulse, adjust its repetition rate and also produce the START signal. The schematic drawing of the transmitter circuit is shown in fig.2. The main sections of the system are:

a) The laser (including the Nd:YAG laser media, the polarizer, the Q-Switch crystal, the cavity mirrors, the flash lamp and a p-i-n diode).

b) The 4.5KV supply.

c) The driver and repetition rate regulator.

d) The laser cooling system.

As can be seen from fig.2, using a Q-Switch and the related driving and oscillating circuits, the repetition rate is adjusted in the range of 1-20Hz. On the other hand, the laser output pulse variation is adjusted to the range 10-15ns, which in turn, causes the laser cavity output power to vary. In accordance to the measured 15mJ energy, the output power could be adjusted from 1.0 to 1.5MW.

The Nd:YAG laser was pumped by a Flash Tube. For the Flash Tube execitation a 4.5KV source was used. Since the cavity power generation is high, the laser cavity need to be cooled by an especial cooling system. The starting signal was produced by a silicon PIN diode having dark current I_d=10nA and a rising time of τ_r=5ns. When triggering the Q-Switch and directing the laser pulse out of the cavity, a current pulse is produced by the diode and implied to the processing section to start the counting.

The range finder receiver consists of two analog and digital sections. The block diagram of the analog section is presented in fig.3. As is shown in the figure, the reflected beam is being detected by an APD having responsivity of $28A/W$ at the wavelength of

$\lambda = 1060nm$. Since the APD is in the current mode of operation , the output signal is amplified by a wide band preamplifier having an input impedance of $50\,\Omega$. The amplifier output signal is given by,

$$V_o = P_{inc}.\Re.Z_t.A_v \qquad (4)$$

where, P_{inc} is the received optical power on the APD, $\Re$ is the APD responsivity, Z_t is the transimpedance gain of the preamplifier and A_v is the amplifier voltage gain. From the designed circuits, the ratio of the output voltage to the power received by the APD equals $1.4MV/W$.

The signal comparison level due to the minimum received power ($10nW$) is considered to be 14mV. This in turn will reduce the system's noise effects. The pulsewidth of the signal is then increased by a monostable and the STOP signal of the counter is implied to the opto-coupler. It then is implied to the digital section of the circuit.

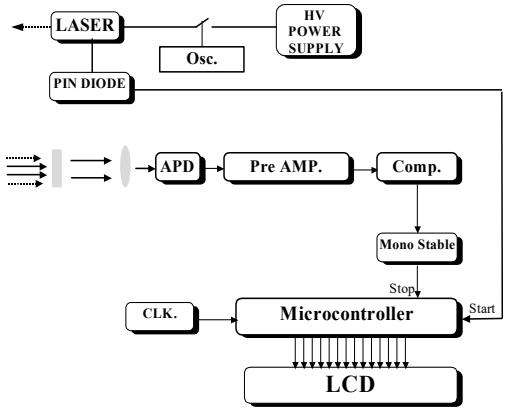

Fig.1 Schematic representation of a time-of-flight range finder system.

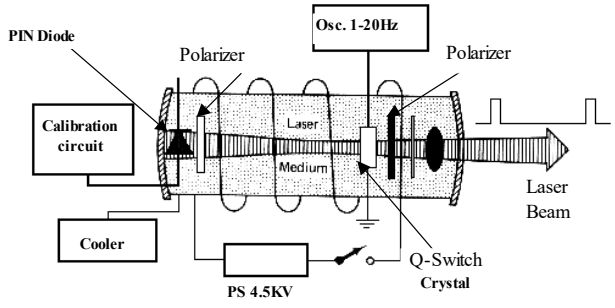

Fig.2 Schematic representation of the transmitter circuit for a TOF laser range finder.

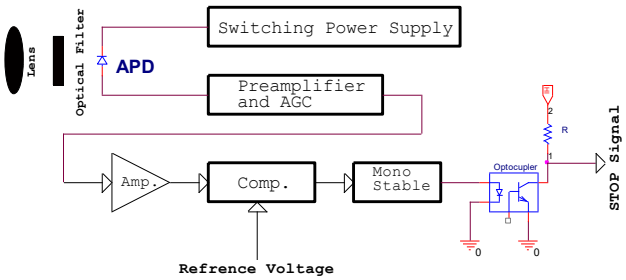

Fig.3 Schematic presentation of the analogue section for the receiver.

Furthermore, it is required that the preamplifier gain to be proportional to the received optical power. This can be accomplished by variation of the APD responsivity with respect to the biasing voltage. By varying the bias in the range 320-351V for this APD, the responsivity varies between 18.5A/W to 123.1A/W. If $\Re$ is the responsivity of the APD and the trans-impedance gain is Z_t, then,

$$A' = \frac{V_o}{P_{inc}} = \Re.Z_t \qquad (5)$$

From this equation, the total gain will vary in the range of 920 KV/W to 6.17MV/W.

The main internal noise is the one created in the receiver STOP channel. Due to the isolation of the analogue section from other parts, the noise effect of the other parts is being curtailed. The switching noise of the 4.5KV flash lamp of the laser is being eliminated by EMI filters. The noise related to the digital section is eliminated by separating the source and the ground from the analogue section of the receiver. However, the main noise related to the receiver channel is the noise of the preamplifier, which is given by,

$$\left\langle i_n^{\,2} \right\rangle = \frac{4KT}{R_{eqi}}\left(\frac{\pi}{2}\Delta f_i\right) \qquad (6)$$

where, k is the Boltzman constant, T is the absolute temperature, R_{eqi} is the preamplifier's input impedance, and Δf_i is the system bandwidth, which is 100MHz. Considering the $50\,\Omega$ impedance for the preamplifier's input, the input current noise is 228nA. The equivalent optical power will then become,

$$P_{inc} = \frac{\langle i_n \rangle}{\Re} \qquad (7)$$

Considering the $28A/W$ responsivity for the APD, the minimum detecting power becomes 12.7nW.

It is well known that signal-to-noise ratio (S/N) is one of the main elements determining the resolution of the system. For our system, the relation between the resolution of the system and the S/N could be presented by

$$\delta_d = \frac{C}{2}.\frac{\langle n \rangle}{dU/dt} = \frac{0.35C}{2B.SNR} \qquad (8)$$

where dU/dt is the slope of the time dependent pulse and $\langle n \rangle$ is the rms noise value. For repetition rate of N ($1<N<15$), Equation (8) changes into,

$$\delta_d = \frac{0.35C}{2\sqrt{N}.B.SNR} \quad (9)$$

On the other hand the signal to noise ratio could be presented as,

$$SNR = \frac{i_S}{i_n} = \frac{M\Re P_{inc}}{\left[2q\left(k_{TP}P_{inc}\Re M^2 F(M) + i_{na}^2\right)\right]^{\frac{1}{2}}} \quad (10)$$

where $k_{TP} = 0.5$, M is the internal gain of the optical detector and F(M) is the excess noise factor. The excess noise factor in terms of the effective ionization ratio can be presented as

$$F(M) = M\left[1-(1-k_{eff})\left(\frac{M-1}{M}\right)^2\right] \quad (11)$$

In this design an appropriate algorithm is designed to reduce the measurement error. Considering the sampling rate 20Hz and the 2sec for refreshing the display, there will be 40 samples in each display. By omitting the out of range data, the measuring error is considerably reduced. Fig.4 presents the measured data for approximate distance of 1.17Km. For primary data the average and standard deviation are 1185.57m and 114.95, respectively. After processing the data change to 1175.23m and 2.92 respectively.

3. FMCW Laser Range Finder

In FMCW-like method, the laser power is frequency modulated with a ramp or sinusoidal wave. The received signal has a time delay with respect to emitted one. If these two signals are mixed, beat frequency will be obtained ($f_{IF}=f_e(t)-f_r(t)$).

As is shown in fig. 5, beat signal (IF) has a transient behavior when slope of the ramp wave changes from upward to downward or vise versa. Except for the unstable zones, the beat frequency can be measured at other points. The distance can be approximated by following equation:

$$d = \frac{F_a.c.T_r}{4.\Delta f} \quad (12)$$

where, F_a is the beat frequency, c is the speed of the light, T_r being the period of the ramp wave and Δf stands for modulation frequency bandwidth.

The electronic components also introduce an additional delay in the received signal which can be accounted for during the calibration process. According to the measuring time intervals, minimum detectable distance corresponds to a half period of beat signal, and $d_{\min} = \frac{c}{4.\Delta f}$. On the other hand, time delay between emitted and received signals can't exceed $\frac{T_r}{2}$ ($\tau_{d\max} = \frac{T_r}{2}$), so $d_{\max} = \frac{c.T_r}{4}$. Practically, the maximum distance is limited by other factors and becomes less than this value.

Figure 6 shows the block diagram of a system that measures distances from 2m to 30m. As shown, frequency modulation is produced by a VCO whose input voltage is a ramp wave. The ramp wave period is 2 kHz and the VCO works linearly from 55 MHz to 130 MHz. At the end of the transmitter section, a laser driver converts the VCO output to the light power. In receiver section, an APD photodetector collects the back scattered light.

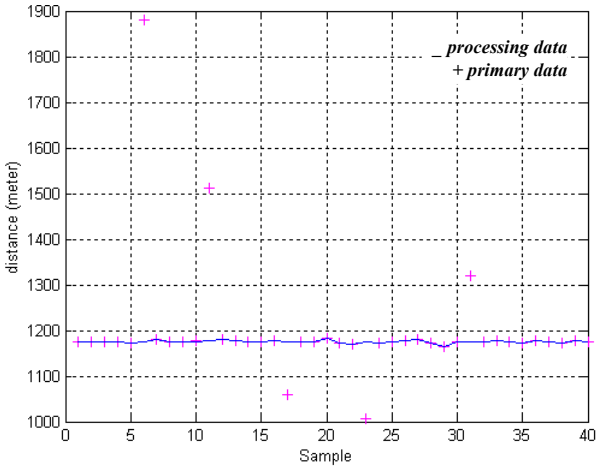

Fig. 4 Measured data for distance of 1.17Km.

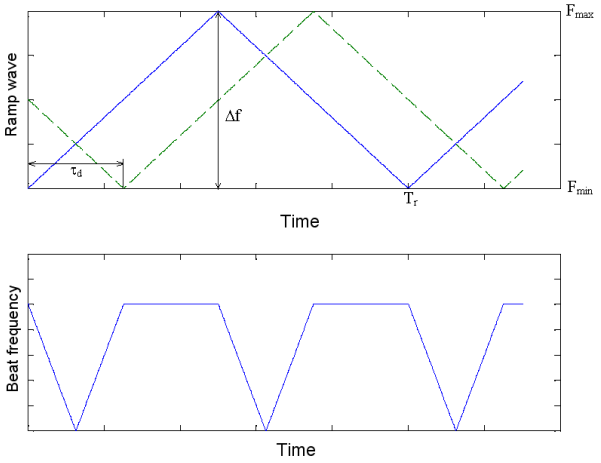

Fig. 5 Ramp wave modulating VCO frequency from F_{min} to F_{max} (top) and resultant beat frequency (bottom).

For maximum and minimum allowable distances we have:

$$F_{a\max} = \frac{4.\Delta f.d_{\max}}{c.T_r} = 60KHz$$
$$F_{a\min} = \frac{4.\Delta f.d_{\min}}{c.T_r} = 4KHz \quad (13)$$

We need a band pass filter with cutoff frequencies lower than 4kHz and higher than 60kHz. The remaining is IF signal and there is one more step to attain the distance data. There are two ways to measure this frequency and convert it to the distance. The first is counting signal cycles during the measuring time interval, and the second is measuring width of the signal to attain period and then $F_a = 1/T_a$. Note that the beat frequency must be measured out of transition zones, and of course a time delay (τ_d) is needed to receive the transmitted signal.

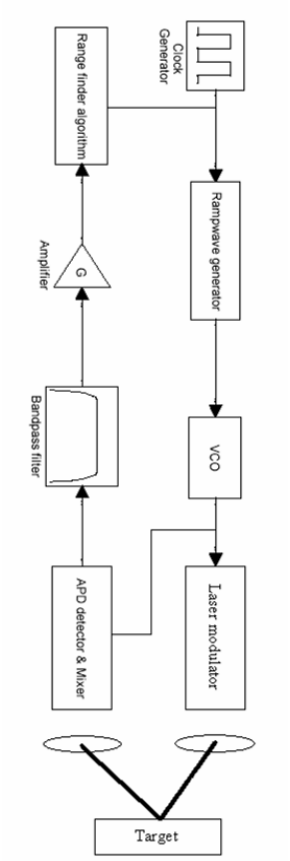

Fig.6 Block diagram of the designed and simulated system

In what follows, we simulate our designed system and obtain resolution for counting and timing methods. Figures 7 and 8 represent waveform and spectrum of the transmitted and mixed signals, respectively, for d=15m.

After the filtering, the beat frequency is converted into distance by using a range finding algorithm. Figures 9 represent distances obtained by counting and timing methods for d=2m and d=30m. We can see that the distance error for counting algorithm is less than 1m for both figures as proved earlier by theoretical principles. As is shown, in counting method, one half period is required to establish the distance data. On the other hand, timing algorithm gives us an error less than 0.036m for d=30m.

4. Phase-Shift Laser Range Finder

In the phase-shift method, the transmitted light intensity is modulated sinusoidally, and the round-trip time is turned into phase shift [4,5,7]. If f_1 is the small signal modulation frequency, the phase shift is presented by,

$$\Delta\phi = \omega_1 \tau_d = 2\pi f_1 \frac{2d}{c} \qquad (14)$$

There are several methods of measuring the resultant phase shift In this research, because the modulation frequency is high, heterodyne technique is being employed. If s_e is the transmission (emission) signal, s_r is the receiving signal, and s_2 being the reference (auxiliary) signal, then,

$$\begin{aligned} s_e &= \hat{S}_e \cos(\omega_1 t) \\ s_r &= \hat{S}_r \cos(\omega_1 t + \phi_d) \\ s_2 &= \hat{S}_2 \cos(\omega_2 t + \psi) \end{aligned} \qquad (15)$$

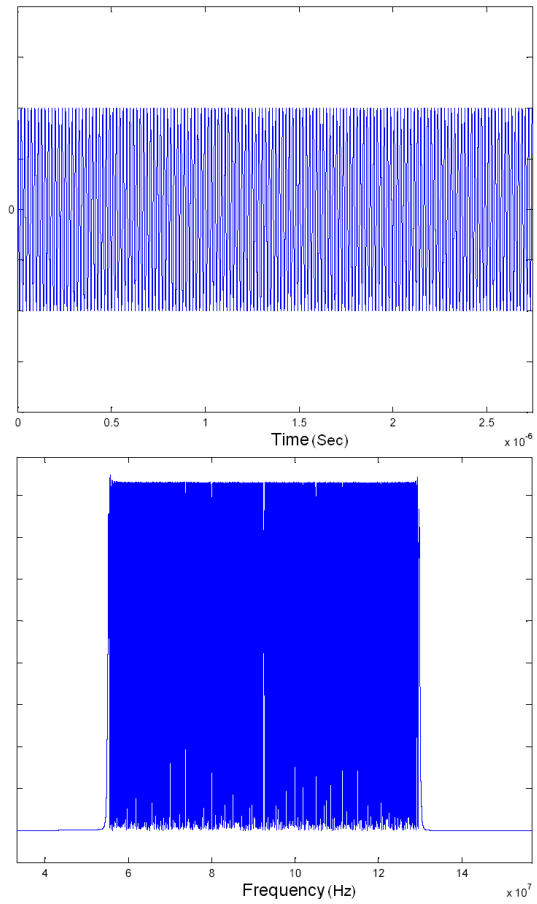

Fig. 7 The waveform (top) and Freq. spectrum (bottom) of transmitted signal.

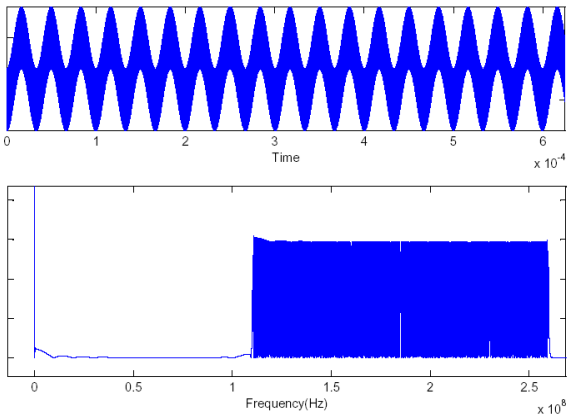

Fig. 8 The waveform and Frequency spectrum of the mixed signal.

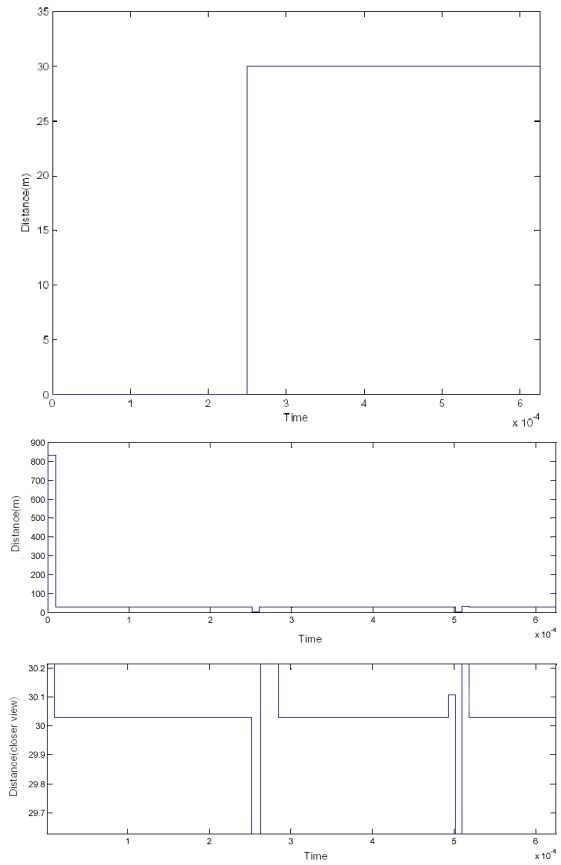

Fig. 9 Distance obtained by full-wave counting (top) and timing (bottom) for d=30m.

According to these equations, it is evident that the transmitting and the receiving frequencies are equal. The term ϕ_d is the signal-phase-delay due to the round trip. The reference signal frequency is f_2 and its phase difference with the main signal is ψ. Based on the heterodyne technique, the multiplication of the transmitting and receiving signals into the auxiliary signal results,

$$X_e = s_e . s_2 = \tfrac{1}{2}\hat{S}_e \hat{S}_2 \{\cos[(\omega_1 - \omega_2)t - \psi] + \cos[(\omega_1 + \omega_2)+\psi]\} \quad (16)$$

$$X_r = s_r . s_2 = \tfrac{1}{2}\hat{S}_r \hat{S}_2 \{\cos[(\omega_1 - \omega_2)t + (\phi_d - \psi)] + \cos[(\omega_1 + \omega_2)+(\phi_d+\psi)]\}$$

Both signals have a differentiation and addition frequencies. Using a low-pass filter to annihilate the addition part,

$$y_e = \hat{Y}_e \cos(\omega_m t - \psi) \quad (17)$$

$$y_r = \hat{Y}_r \cos(\omega_m t + \phi_d - \psi)$$

where, ϕ_d (in radian) is the phase difference between the tow final signals. It is equal to that considered for the case of the round trip. Figure 10 shows the general block diagram of a phase-shift laser altimeter system, giving a primary insight to the important sections of the system.

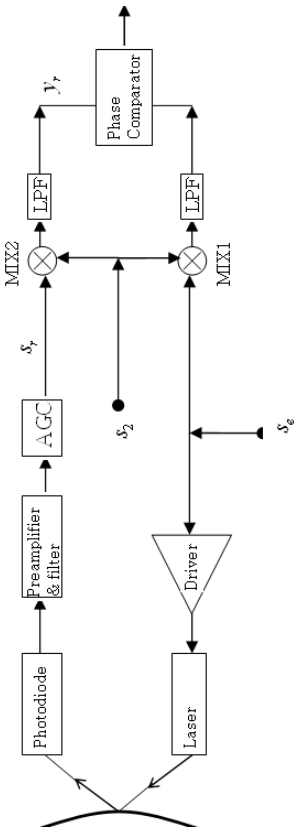

Fig. 10 The block diagram of a phase shift laser altimeter system.

Since the frequency of the designed circuit is relatively low, the system error (δ_d) due to the cross-talk, as a function of the distance could be expressed as:

$$\delta_d = \frac{C}{2}\cdot\frac{\Psi_0 - \alpha_0}{2\pi f_1} = -\frac{C}{4\pi f_1}\arctan\frac{\sin[\theta_0 - \frac{4\pi}{C}f_1(r - r_{\max})]}{\frac{A_0}{B}.(\frac{r_{\max}}{r})^2 + \cos[\theta_0 - \frac{4\pi}{C}f_1(r - r_{\max})]} \quad (18)$$

In this equation, $\Psi_0 - \alpha_0$ is the phase difference between the working and the measured signals, and A_0 / B is the ratio of the main signal (the signal related to the photons) to the leakage one. Selecting the modulation frequency with respect to the final divider as f_1=371.838 kHz, and the related maximum distance of $r_{\max}$=403m, and assuming a maximum phase divination between the working and the leakage signals to be $\theta_0 = 90^o$, one could measure the deviation of the distance due to cross-talk for different distances. A graph of the distance error variation for leakages as a function of distance for the ratio of A_o /B equal to 10dB, 50dB, and 100dB is shown fig.12. As can be seen from the figure, by increasing A_o /B, one can decrease the measured error considerably.

By shielding the system properly, and decreasing the laser diode's driving voltage amplitude, the coupling capacitor effect was decreased

considerably. Since increasing the cutoff frequency could decrease the induced coupling, the input impedance of the current to voltage converter was also relatively decreased. Of course, care should be taken to not decrease the detector gain too much. A further decrease of cross-talk was possible by isolation of the transmitter and receiver power supplies. In general, considering the A/B =100 dB in the simulation, the maximum cross-talk error is less than 0.2 percent in the worst condition.

Another possible error of the system is the error created by the small variation in the oscillator frequency. To reduce or possibly eliminate this error, one could create both signals by a single oscillator. For example, an oscillator with frequency f, is employed as the main oscillator. Designing a synthesizer with coefficient of 1.01, a frequency of 1.01f can be assigned for the local oscillator.

In this case, the IF frequency becomes 0.01f. However, it should be noted that, this will increase the hardware considerably. Hence, in this system, the measurement of IF is used to decrease the error. In fig.12 the error measurement difference with and without IF measurement is shown. As can be seen, the error resulted from the frequency shift has approached to zero value. Hence, one can practically conclude that, in a 2 to 400 m range, the error is less than 1.2 percent.

5. Comparison

Table 1 depicts the measured and calculated data of the three above discused systems. It is clearly seen that the phase-shift method has the best detection ability. However, the accuracy to the maximum range ratio is best in TOF.

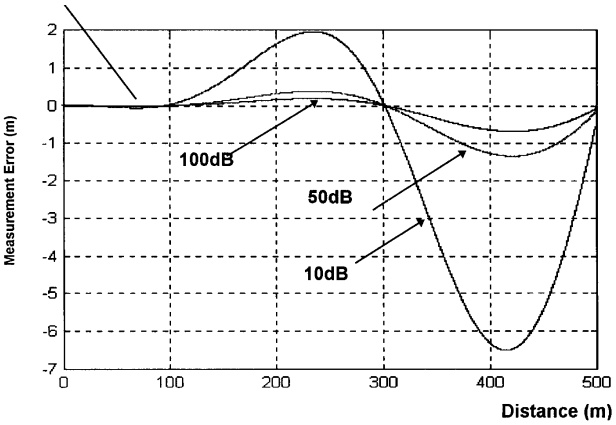

Fig. 11 A graph of the distance error variation for leakages as a function of distance for A_o / B=10, 50 and 100dB.

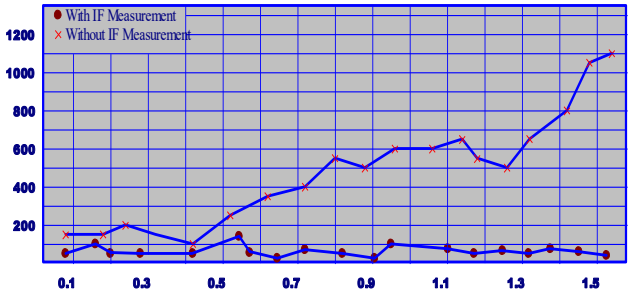

Fig. 12 The error measurement difference with and without IF measurement.

Table 1 Comparison of TOF, FMCW and Phase Shift laser range finding methods.

Range Finding Methods	TOF	FMCW	Phase-Shift
Laser Source	Nd:YAG, Q-Switch	Semiconductor	Semiconductor
Power	1.5MW	3mW	10mW
Wavelength	1064nm	650nm	1100nm
Detector	APD	APD	APD
Range	300-20km	2-30m	2-400m
Sampling Rate	1-20Hz	4kHz	52Hz
Minimum Detectable Power	12.7nW	200nW	23pW
Accuracy	5m	36mm	21mm
Oscillator Frequency	30MHz	4-60MHz	1MHz
Driving Power	Three Phase	Single Phase	Single Phase
Laser Driving Waveform	Pulse	Ramp	Sinusoidal
Cost	Expensive	Low Cost	Low Cost
Structural Complexity	Simple	Complex	Complex
Distance Measuring Equation	$d=\frac{CN}{2f_{clk}}$	$d=\frac{F_a C.T_r}{4\Delta f}$	$d=\frac{C}{4f}$

6. Conclusion

TOF and Phase-Shift range-finding systems were designed and implemented. FMCW-like system was also designed and simulated. According to their distinct characteristics, their applications are classified. Hence, based on the classification, a user can easily choose the proper system.

References

[1] B.Zagar, 'A Laser-Interferometer Measuring Displacement with Nanometer Resolution', IEEE.Trans.Inst.measu., Vol.43, No.2,PP.332-336 (1994).

[2] J.C.Martinez, 'A robust photo-interferometric technique to obtain the refractive index and thickness of non-absorbing stand-alone films', Meas.Sci.Tech.11,PP.1138-1144 (2000).

[3] U.Minoni and L.Rovalti , 'High performance front-end electronic for frequency-modulated continuous-wave interferometers', IEEE. Trans.Inst.measu., Vol.48, No.6 ,PP.1191-1196 (1999).

[4] I.Fujima, S.Iwasaki and K.Seta , 'High-Resolution Distance Meter using Optical Intensity Modulation at 28 GHz' ,Meas.Sci.Tech.,PP.1049-1052 (1998).

[5] G.Bazin and B.Journet, 'A New Laser Range-Finder Based on FMCW-Like Method', IEEE. Ins. Measu. Tech. Conference, Belgium, June 4-6,PP.90-93 (1996).

[6] G.Barwood and R.Rowley, 'High-Accuracy Length Meterology using Multiple-Stage Swept-Frequency Interferometry with Laser Diode', Measu. Sci. Tech. 9,PP.1036-1041 (1998).

[7] M.Vered and A.Aire, 'Distance Measurement Using Tow Frequency-Stabilized Nd:YAG Lasers', Appl. Opt. 35, 1996, PP.3010-15.

[8] T.Kawakami and M.Endo, 'Adaptive Multiferequency Modulation Method for an Advanced Laser Range Finder', IEEE. Trans. Inst. measu., Vol.43, No.6, 1994, PP.857-860.

[9] Geo-Qing Wei and G.Hirzinger, 'Active Self-Calibration of Hand-Mounted Laser Range Finders', Proceeding of the 1997 IEEE, April 1997, PP.2789-2794.

[10] K.maatta, 'Profiling of hot surfaces by pulsed time of flight laser range finder techniques', Applied Optics, Vol. 32, No.27, 1993, PP. 5334-5342.

[11] F.Refaat,'Characterization of advanced avalanche photodiode for water vapor lidar receivers', NASA/TP2000, July 2000.

[12] P.Bhattacharya,'Semiconductor Optoelectronic Devices and optics' ,Prentice Hall, Second Edition , 1997.

[13] Ari. Kilpela, 'Pulsed Time-of-Flight Laser Range Finder Techniques for Fast, High Precision Measurement Applications', OULU, 2004.